Huang et al. Nanoscale Research Letters (2017) 12:310
DOI 10.1186/s11671-017-2088-7

Nanoscale Research Letters

NANO EXPRESS Open Access

Fabrication of TiO_2 Nanosheet Aarrays/Graphene/Cu_2O Composite Structure for Enhanced Photocatalytic Activities

Jinzhao Huang[1*], Ke Fu[1], Xiaolong Deng[1], Nannan Yao[1] and Mingzhi Wei[2]

Abstract

TiO_2 NSAs/graphene/Cu_2O was fabricated on the carbon fiber to use as photocastalysts by coating Cu_2O on the graphene (G) decorated TiO_2 nanosheet arrays (NSAs). The research focus on constructing the composite structure and investigating the reason to enhance the photocatalytic ability. The morphological, structural, and photocatalytic properties of the as-synthesized products were characterized. The experimental results indicate that the better photocatalytic performance is ascribed to the following reasons. First, the TiO_2 NSAs/graphene/Cu_2O composite structure fabricated on the carbon cloth can form a 3D structure which can provide a higher specific surface area and enhance the light absorption. Second, the graphene as an electron sink can accept the photoelectrons from the photoexcited Cu_2O which will reduce the recombination. Third, the TiO_2 nanosheet can provide more favorable carrier transportation channel which can reduce the recombination of carriers. Finally, the Cu_2O can extend the light absorption range.

Keywords: TiO_2 nanosheet arrays, Graphene, Cu_2O, Heterostructure, Photocatalysis

Background

Recently, application of semiconductor photocatalyst titanium dioxide (TiO_2) in environmental purification has attracted great attention owing to its tremendous advantages, such as stability, nontoxicity, and low cost [1–3]. Based on the fact that photocatalytic reactions mainly take place on the surfaces of the photocatalysts, the morphology is the crucial factor to determine the efficiency [4]. Up to now, many efforts have been made to fabricate TiO_2 nanocrystals, nanowires, nanorods, and nanotubes [5–8]. However, the application of TiO_2 nanosheet arrays with larger specific surface area in photocatalytic degradation is rarely reported. Especially, TiO_2 nanosheet arrays grown on the carbon cloth can construct three-dimensional (3D) structures to improve the specific surface area.

Unfortunately, the wide bandgap of TiO_2 limits the effective absorption of visible light [9]. In order to overcome the shortcoming, one strategy is to modify TiO_2 with narrow bandgap semiconductors [10–12]. Among them, cuprous oxide (Cu_2O) with narrow bandgap can be a promising candidate for expanding the absorption spectra range. [13–18] Moreover, the built-in electric field between P-type Cu_2O and N-type TiO_2 can accelerate the separation of carriers.

However, the poor interfacial feature between different semiconductors directly influences the separation efficiency of carriers. Therefore, the interfacial optimization is an effective way to enhance photocatalytic degradation efficiency [19, 20]. The previous researches indicate that graphene (G) shows excellent interfacial optimization function between different semiconductors due to its high conductivity and two-dimensional structure, which facilitates the interfacial contact and carrier transportation [21–25]. However, it is difficult to make graphene well disperse between different semiconductors. In this paper, a modified method is applied to fabricate the homogeneously dispersed G between TiO_2 nanosheet and Cu_2O.

In this study, the composite structure of TiO_2 NSAs/G/Cu_2O has been prepared (Fig. 1). The significant enhancement of photocatalytic activities was observed, and the corresponding results were analyzed. The

* Correspondence: ss_huangjinzhao@ujn.edu.cn
[1]School of Physics and Technology, University of Jinan, Jinan 250022, Shandong Province, People's Republic of China
Full list of author information is available at the end of the article

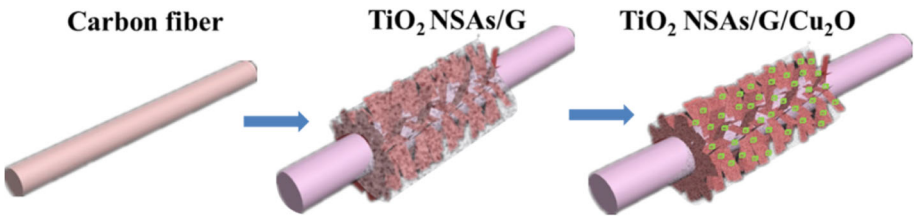

Fig. 1 Schematic illustration for the preparation of TiO_2 NSAs/G/Cu_2O

proposed mechanism of the photocatalytic degradation was also discussed. As we know, there are no related reports on TiO_2 NSAs/G/Cu_2O photocatalysts up to now, so and thus it will be a meaningful reference for designing and fabricating this kind of photocatalyst used in photocatalytic degradation.

Methods

Preparation of TiO_2 NSAs/G/Cu_2O

The fabrication of TiO_2 NSAs is the following. TiO_2 sol was prepared using a previously reported method [10]. In brief, TiO_2 seed layer was deposited on carbon cloth (2 cm × 3 cm) by immersing in TiO_2 sol for 10 min. Then, the seed layer was calcined at 400 °C for 1 h. The Teflon-lined stainless steel autoclave (100 mL in volume) filled with 40 mL of aqueous solution of 10 M NaOH and 0.2 g of activated carbon was placed in an oven at 180 °C for 24 h. After the autoclave cooled down to room temperature, the prepare samples were rinsed with DI water to remove the residual activated carbon, followed by soaking with 0.1 M hydrochloric acid for 1 h, then washed to neutral with DI water.

For the composite structure of TiO_2 NSAs/G, 0.2 g of graphene replacing activated carbon was added into the Teflon-lined stainless steel autoclave ethanol solution.

Cu_2O layer was deposited by the following procedures. 2.3 mmol of $Cu(CH_3COO)_2$ and 2.3 mmol of CH_3CONH_2 were dissolved into 100 mL of diethylene glycol (DEG) under ultrasonication to prepare the reaction solution. Then, TiO_2 NSAs or TiO_2 NSAs/G substrate was immersed into the solution. Subsequently, it was heated to 120° under magnetic stirring and kept at this temperature for 6 h. After cooling down to room temperature in air, TiO_2 or TiO_2 NSAs/G substrate coated with Cu_2O was washed with absolute ethanol and DI water for five times in sequence and dried in air.

Characterization

The morphologies of the samples were investigated by a field emission scanning electron microscopy (FE-SEM, Quanta FEG250). The crystal structure of samples was examined by X-ray diffraction (XRD, D8 Advance) with Cu K_α at $\lambda = 0.15406$ nm radiation. XPS spectra were recorded on a Thermo Fisher ESCALAB 250Xi system with Al Kα radiation, operated at 150 W. The absorption spectrum of the samples was measured using a UV–vis spectrophotometer (TU-1901). The Raman spectrum of the sample was characterized by Raman spectroscopy (LabRAM HR800).

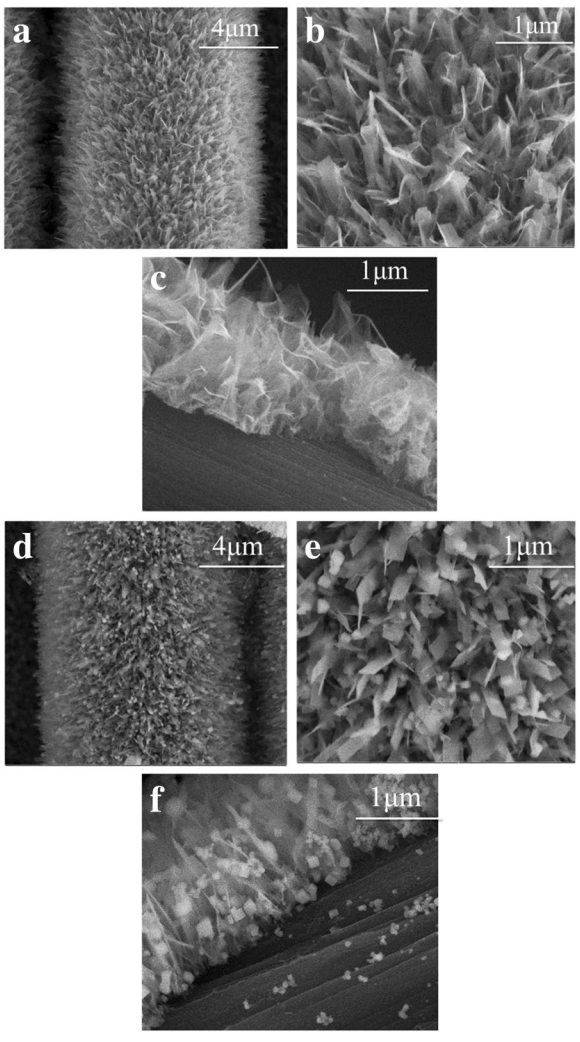

Fig. 2 SEM images of **a**–**c** TiO_2 NSAs with different magnification, **d**–**f** TiO_2 NSAs/G/Cu_2O with different magnifications

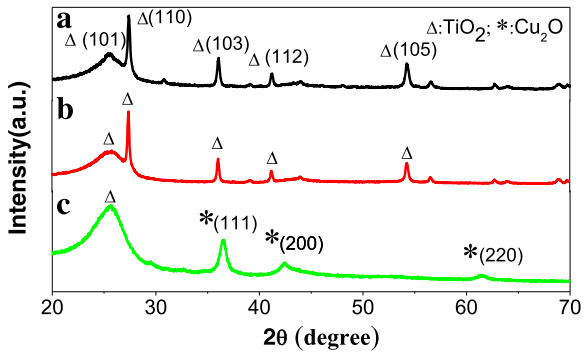

Fig. 3 XRD patterns of **a** TiO_2 NSAs, **b** TiO_2 NSAs/G, and **c**TiO_2 NSAs/G/Cu_2O

Photoelectrochemical Measurement

Photocurrent density was measured using an electrochemical workstation (CS2350) in a three-electrode electrochemical cell with 1 M Na_2SO_4 as the electrolyte, in which the as-prepared samples were acted as the working electrode, Pt and Ag/AgCl electrode were used as the counter and reference electrodes, respectively. The *I*–*t* curve was recorded under Xe lamp (153 mW/cm^2) irradiation.

Measurement of Photocatalytic Activity

The photocatalytic activity was evaluated toward the photodegradation of RhB. A 500 W Xe lamp was used as the light source. The samples with same size 2 cm × 3 cm were placed into 20 ml RhB solution (10 mg/L). After irradiation for a designated time (30 min), 3 mL of RhB solution was taken out to identify the concentration of RhB using UV–vis spectrophotometer (TU-1901). All of these measurements were carried out at room temperature.

Results and Discussion

Figure 2a–c, the obtained TiO_2 NSAs characterized by FE-SEM, shows that the uniform TiO_2 NSAs with about 40–60 nm in width and 1.5 μm in height vertically grew on the surface of carbon cloth. These results illustrate that the morphology in favor of the enhancement of photocatalytic performance. As shown in Fig. 2d–f, Cu_2O particles have been successfully deposited on the

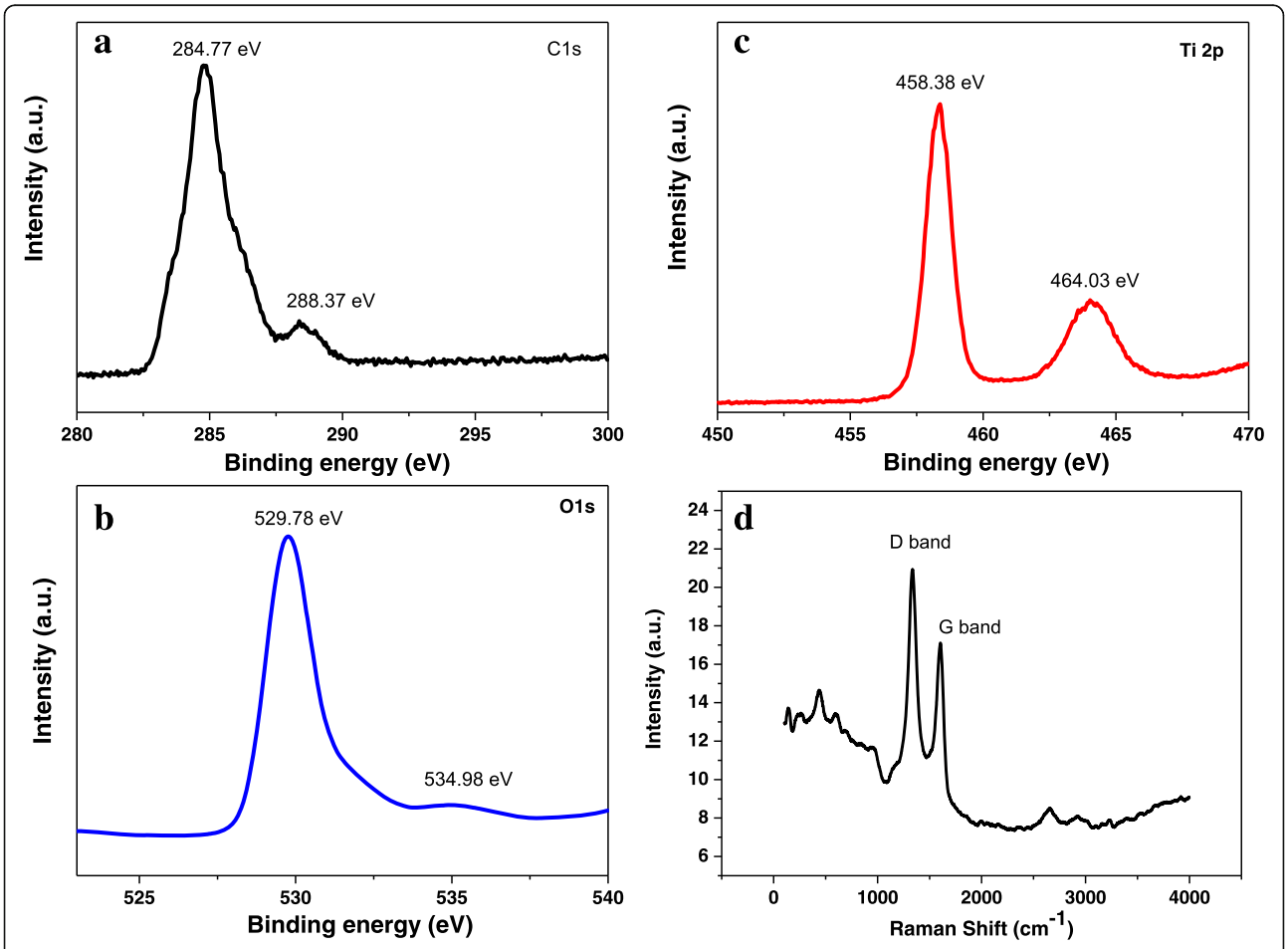

Fig. 4 XPS spectra of **a** C 1s, **b** O 1s, **c** Ti 2p of TiO_2 NSAs/G, and **d** Raman spectra of TiO_2 NSAs/G

surface of the nanosheets. Unfortunately, G cannot be directly observed in Fig. 1d, e, though it could be confirmed by XPS measurement.

XRD patterns were performed to investigate the crystal phase structure of photocatalyst. The XRD patterns of TiO_2 NSAs, TiO_2 NSAs/G, and TiO_2 NSAs/G/Cu_2O are shown in Fig. 3. For TiO_2 NSAs (curve a), five distinctive peaks match well with TiO_2. In curve b (for TiO_2 NSAs/G), there are the same diffraction peaks with curve a. The phase on G is not detected because the content is low. From the curve c (TiO_2 NSAs/G/Cu_2O), the diffraction peaks on Cu_2O are observed.

X-ray photoelectron spectroscopy (XPS) was used to confirm the existence of G. The XPS survey spectrum of TiO_2 NSAs/G composite shows the elements C, O, and Ti (Fig. 4a–c). The presence of these elements proves the method to fabricate TiO_2 NSAs/G composite is feasible. XPS spectrum of C1s located at 284.77 eV can be corresponded to carbon-containing species on the surface, which is the dominant existence form (Fig. 4a). Moreover, the 288.37 eV indicates the tiny existence of C–O bond. The peak located at 529.78 eV is related to the oxygen bonded with metal as Ti–O, and the 534.98 eV is the adsorbed oxygen or hydroxyl species (Fig. 4b). It can be seen that the spectra of catalysis showed two peaks at 458.38 and 464.03 eV. These peaks can be assigned to 3d5/2 and 3d3/2 spin orbital components of Ti^{4+} species (Fig. 4c) [26, 27]. In order to confirm the existence of graphene, furtherly, the Raman spectrum was characterized. The typical Raman spectra of TiO_2 NSAs/G are shown in Fig. 4d. There are two typical Raman peaks corresponding to the typical D band and G band of graphene, respectively.

The photocatalytic properties of the as-obtained samples were investigated by decomposition of RhB (Fig. 5a). Before irradiation started, the system was kept in dark for 1 h to reach the adsorption–desorption equilibrium. There is almost no change in the concentration of the solution when RhB solution is irradiated without any catalysts. After 180 min, the degradation ratio of RhB was almost 80% in the presence of TiO_2 NSAs/G/Cu_2O, whereas 50 and 40% of RhB was decomposed by TiO_2 NSAs and TiO_2 NSAs/ Cu_2O, respectively. All of these measurements show that TiO_2 NSAs/G/Cu_2O exhibits more prominent photocatalytic activity compared with other samples. A very important reason for the advantage of TiO_2 NSAs/Cu_2O on the photodegradation of RhB is that Cu_2O plays a significant role in extending light absorption spectrum. In addition, TiO_2 NSAs/G/Cu_2O exhibits a better photocatalytic activity than TiO_2 NSAs/Cu_2O which results from the presence of graphene. The graphene as an electron sink to accept the photoelectrons from the photoexcited Cu_2O will reduce the recombination of photoelectron-hole pairs, resulting in a higher photocatalytic activity. The stability of the TiO_2 NSAs/G/Cu_2O was carried out, and the results (Fig. 5b) show that TiO_2 NSAs/G/Cu_2O has good stability.

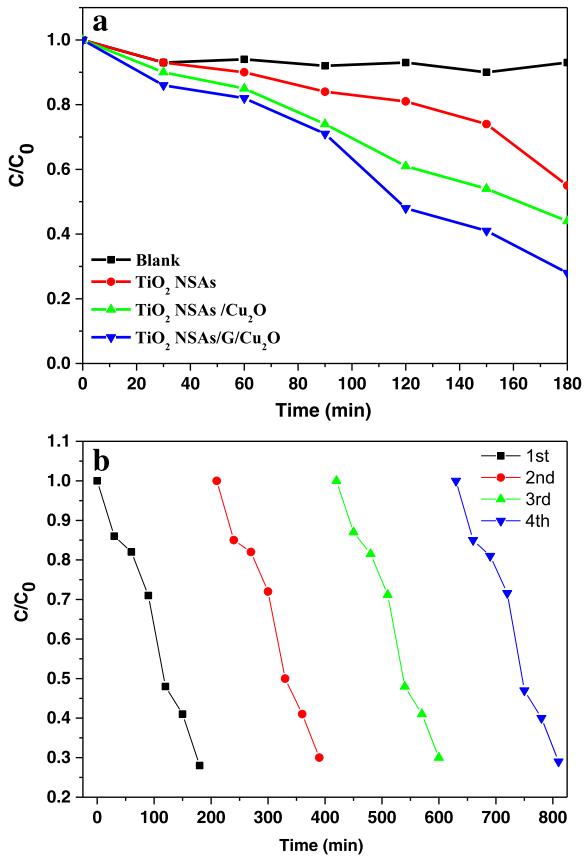

Fig. 5 **a** Photocatalytic degradation of RhB in the presence of various catalysts. **b** Recycle of TiO_2 NSAs/G/Cu_2O under Xe lamp irradiation

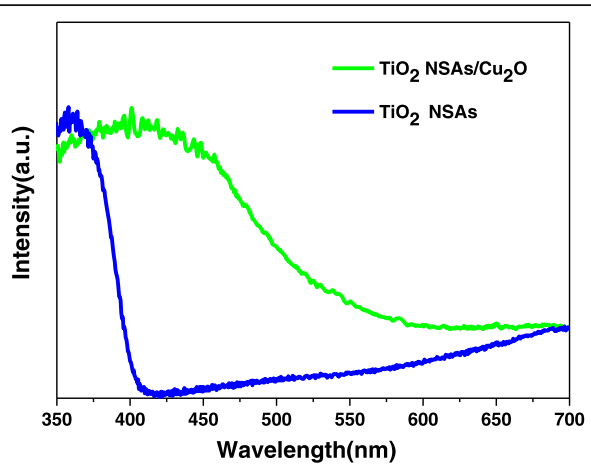

Fig. 6 UV–vis absorption spectra of TiO_2 NSAs and TiO_2 NSAs/Cu_2O

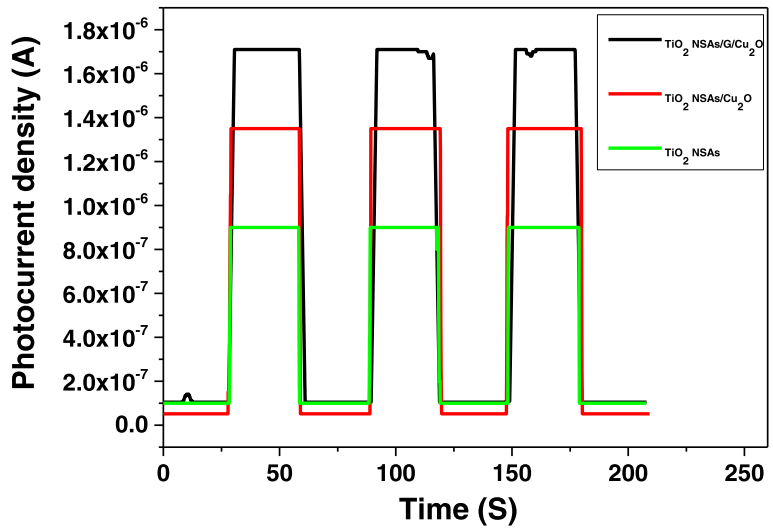

Fig. 7 Photoinduced *I–t* curves of different samples

Generally, responding ability to light is one of the most important factors for evaluating photocatalytic performance. Therefore, UV–vis absorption spectra of samples were characterized as shown in Fig. 6. The absorption of TiO_2 NSAs is located in the UV region. Compared with TiO_2 NSAs, the absorption edge of TiO_2 NSAs/Cu_2O shows redshift. This larger absorption would result in the improvement of the photocatalytic property of TiO_2 NSAs/Cu_2O.

To further understand the improvement of photocatalytic activity, the *I–t* response of TiO_2 NSAs, TiO_2 NSAs /Cu_2O, and TiO_2 NSAs/G/Cu_2O were observed, as shown in Fig. 7. It can be found that TiO_2 NSAs/G/Cu_2O exhibits enhanced photocurrents compared with TiO_2 NSAs and TiO_2 NSAs/Cu_2O. The higher photocurrent density of TiO_2 NSAs/G/Cu_2O indicates an enhanced light absorption and higher separation efficiency of photogenerated electrons and holes.

The improved photocatalytic property of TiO_2 NSAs/G/Cu_2O may be attributed to the following factors. First, the introduction of Cu_2O can extend the light absorption range, and thus, the photocatalytic activities are enhanced. Second, the limitation of carrier recombination is a key factor to enhance the photocatalytic property. The graphene as an electron sink can accept the photoelectrons from the photoexcited Cu_2O which will reduce the recombination. Besides, TiO_2 nanosheet structure can provide more favorable carrier transportation channel. Third, the better photocatalytic property can take advantage of large specific surface area. TiO_2 NSAs/G/Cu_2O structure fabricated on the carbon cloth can form a 3D structure which can provide a higher specific surface area. The high surface area of the 3D structure allows not only more surfaces to be reached by the incident light but also more sites on the surface for the adsorption and photodegradation of RhB, which results in enhanced photocatalytic performance. Finally, the 3D structure can enhance the photon utilization efficiency. The structure allows a great number of the photons to penetrate deep inside the photocatalyst, and most photons are trapped within the 3D structure until being completely absorbed.

The corresponding mechanism of electron transfer has been illustrated in Fig. 8. Both TiO_2 and Cu_2O can be photoexcited under the light irradiation. Because the E_{VB} of TiO_2 is more positive than that of Cu_2O, holes in the VB of TiO_2 can migrate to the VB of Cu_2O by the interface. Similarly, the E_{CB} of Cu_2O is higher than that of TiO_2, so the electrons in the CB of Cu_2O can transfer

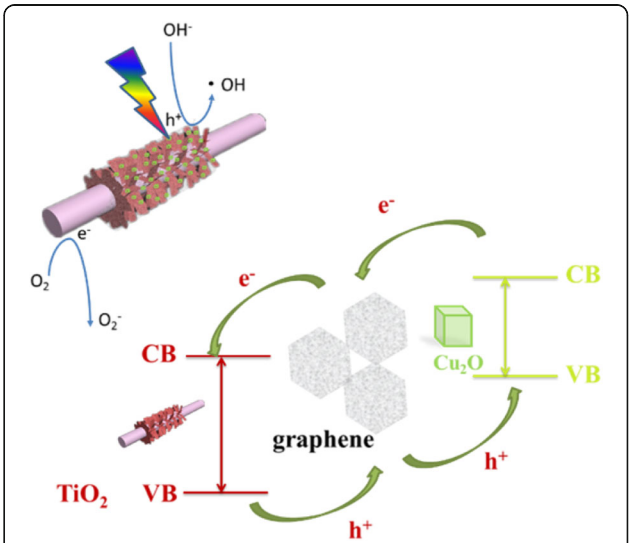

Fig. 8 The possible photocatalytic mechanisms of TiO_2 NSAs/G/Cu_2O

to the CB of TiO_2. More importantly, graphene as electronic exchange medium can promote electron transfer ability between Cu_2O and TiO_2.

Conclusions

In summary, the novel 3D TiO_2 NSAs/G/Cu_2O structure is prepared via a simple and efficient method. Importantly, the composite structure exhibits excellent photocatalytic degradation properties. The enhanced performance can be ascribed to its extended light absorption range, large specific surface area, enhanced photon utilization efficiency, improved charge transfer efficiency and suppressed photoelectron-hole recombination. Furthermore, the photocatalysts grown on carbon cloths make the collection and recycle of photocatalysts much easier.

Acknowledgements

This work was supported by the Natural Science Foundation of Shandong Provience (Grant Nos. ZR2016FM30, ZR2016JL015), the Science-Technology Program of Higher Education Institutions of Shandong Province (Grant No. J14LA01), the Graduate Innovation Foundation of University of Jinan, GIFUJN, (Grant No. YCXS15006), the Open Project Program of Key Laboratory for Photonic and Electric Bandgap Materials, Ministry of Education, Harbin Normal University (Grant No. PEBM201505), and National Natural Science Foundation of China (Grant Nos. 51672109, 61504048, 21505050).

Authors' contributions

Y.N.N. and H.J.Z. designed the experiments. Y.N.N. and F.K. performed the experiments. D.X.L. performed the SEM observations. Y.N.N., H.J.Z., D.X.L., and W.M.Z. discussed and commented on the experiments and results and wrote the paper. All authors read and approved the final manuscript.

Competing interests

The authors declare that have no competing interests.

Publisher's Note

Author details

[1]School of Physics and Technology, University of Jinan, Jinan 250022, Shandong Province, People's Republic of China. [2]School of Material Science and Engineering, Qilu University of Technology, Jinan 250353, Shandong Province, People's Republic of China.

Received: 8 March 2017 Accepted: 18 April 2017
Published online: 26 April 2017

References

1. Schneider J, Matsuoka M, Takeuchi M, Zhang J, Horiuchi Y, Anpo M, Bahnemann DW (2014) Understanding TiO2 photocatalysis: mechanisms and materials. Chem Rev 114:9919–9986
2. Zhang Z, Huang Y, Liu K, Guo L, Yuan Q, Dong B (2015) Multichannel-improved charge-carrier dynamics in well-designed hetero-nanostructural plasmonic photocatalysts toward highly efficient solar-to-fuels conversion. Adv Mater 27:5906–5914
3. Fu K, Huang J, Yao N, Xu X, Wei M (2015) Enhanced photocatalytic activity of TiO_2 nanorod arrays decorated with CdSe using an upconversion TiO_2: Yb^{3+}, Er^{3+} thin film. Ind Eng Chem Res 54:659–665
4. Tian J, Hao P, Wei N, Cui H, Liu H (2015) 3D Bi_2MoO_6 nanosheet/TiO_2 nanobelt heterostructure: enhanced photocatalytic activities and photoelectochemistry performance. ACS Catal 5:4530–4536
5. Wang J, Ji G, Liu Y, Gondal MA, Chang X (2014) Cu_2O/TiO_2 heterostructure nanotube arrays prepared by an electrodeposition method exhibiting enhanced photocatalytic activity for CO_2 reduction to methanol. Catal Commun 46:17–21
6. Yan W, He F, Gai S, Gao P, Chen Y, Yang P (2014) A novel 3D structured reduced graphene oxide/TiO_2 composite: synthesis and photocatalytic performance. J Mater Chem A 2:3605–3612
7. Huang J, Fu K, Yao N, Deng X, Ding M, Shao M, Xu X, Wei M (2016) Enhanced photocatalytic performance using one dimensional ordered TiO_2 nanorods modified by graphene oxide. J Nanosci Nanotechnol 16:14771482
8. Wei X, Shao C, Li X, Lu N, Wang K, Zhang Z, Liu Y (2016) Facile in situ synthesis of plasmonic nanoparticles-decorated g-C_3N_4/TiO_2 heterojunction nanofibers and comparison study of their photosynergistic effects for efficient photocatalytic H_2 evolution. Nanoscale 8:11034–11043
9. Yao N, Huang J, Fu K, Liu S, E D, Wang Y, Xu X, Zhu M, Cao B (2014) Efficiency enhancement in dye-sensitized solar cells with down conversion material ZnO: Eu^{3+}, Dy^{3+}, J Power Sources 267:405–410
10. Fu K, Huang J, Yao N, Deng X, Xu X, Li L (2016) Hybrid nanostructure of TiO_2 nanorod arrays/Cu_2O with a $CH_3NH_3PbI_3$ interlayer for enhanced photocatalytic activity and photoelectrochemical performance. RSC Adv 6: 57695–57770
11. Huang J, Liu S, Kuang L, Zhao Y, Jiang T, Liu S, Xu X (2013) Enhanced photocatalytic activity of quantum-dot-sensitized one-dimensionally-ordered ZnO nanorod photocatalyst. J Environ Sci 25:2487–2491
12. Dutta SK, Mehetor SK, Pradhan N (2015) Metal semiconductor heterostructures for photocatalytic conversion of light energy. J Phys Chem Lett 6:936–944
13. Hara M, Kondo T, Komoda M, Ikeda S, Kondo J, Domen K, Hara M, Shinohara K, Tanaka A (1998) Cu_2O as a photocatalyst for overall water splitting under visible light irradiation. Chem Commun 3:357–358
14. Paracchino A, Laporte V, Sivula K, Grätzel M, Thimsen E (2011) Highly active oxide photocathode for photoelectrochemical water reduction. Nat Mater 10:456–461
15. Li C, Li Y, Delaunay J (2013) A novel method to synthesize highly photoactive Cu_2O microcrystalline films for use in photoelectrochemical cells. ACS Appl Mater Interfaces 6:480–486
16. Tilley S, Schreier M, Azevedo J, Stefik M, Graetzel M (2014) Ruthenium oxide hydrogen evolution catalysis on composite cuprous oxide water-splitting photocathodes. Adv Funct Mater 24:303–311
17. Li C, Hisatomi T, Watanabe O, Nakabayashi M, Shibata N, Domen K, Delaunay J (2015) Positive onset potential and stability of Cu_2O-based photocathodes in water splitting by atomic layer deposition of a Ga_2O_3 buffer layer. Energy Environ Sci 8:1493–1500
18. Li C, Hisatomi T, Watanabe O, Nakabayashi M, Shibata N, Domen K, Delaunay J (2016) Simultaneous enhancement of photovoltage and charge transfer in Cu_2O-based photocathode using buffer and protective layers. Appl Phys Lett 109:033902
19. Fan W, Yu X, Lu H, Bai H, Zhang C, Shi W (2016) Fabrication of TiO_2/RGO/Cu_2O heterostructure for photoelectrochemical hydrogen production. Appl Catal Environ 181:7–15
20. Fu K, Huang J, Yao N, Xu X, Wei M (2016) Enhanced photocatalytic activity based on composite structure with down-conversion material and graphene. Ind Eng Chem Res 55:1559–1565
21. Li X, Yu J, Jaroniec M (2016) Hierarchical photocatalysts. Chem Soc Rev 45: 2603–2636
22. Li J, Wu N (2015) Semiconductor-based photocatalysts and photoelectrochemical cells for solar fuel generation: a review. Catal Sci Technol 5:1360–1384
23. Li X, Yu J, Wageh S, Al-Ghamdi AA, Xie J (2016) Graphene in photocatalysis: a review. Small 12:6640–6696
24. Ge M, Li S, Huang J, Zhang K, Al-Deyab SS, Lai Y (2015) TiO_2 nanotube arrays loaded with reduced graphene oxide films: facile hybridization and promising photocatalytic application. J Mater Chem A 3:3491–3499
25. Li Q, Li X, Wageh S, Al-Ghamdi AA, Yu J (2015) CdS/graphene nanocomposite photocatalysts. Adv Energy Mater 5:1500010
26. Bhosale RR, Pujari SR, Muley GG, Patil SH, Patil KR, Shaikh MF, Gambhire AB (2014) Solar photocatalytic degradation of methylene blue using doped TiO2 nanoparticles. Sol Energy 103:473–479
27. Alsawat M, Altalhi T, Gulati K, Santos A, Losic D (2015) Synthesis of carbon nanotube–nanotubular titania composites by catalyst-free CVD Process: insights into the formation mechanism and photocatalytic properties. ACS Appl Mater Interfaces 7:28361–28368